Electronic Supplementary Material (ESI) for Nanoscale.

Supplementary Information

Reducing ZnO Nanoparticle Cytotoxicity by Surface Modification

Mingdeng Luo[1], *Cenchao Shen*[2], *Bryce N. Feltis*[2, 3], *Lisandra L. Martin*[1], *Anthony E. Hughes*[4], *Paul F.A. Wright*[2] *and Terence W. Turney*[3*]

[1]School of Chemistry, Monash University, Clayton VIC 3800, Australia, [2]School of Medical Sciences, and NanoSafe Australia, RMIT University, Bundoora VIC 3083, Australia, [3] Department of Materials Engineering, Monash University, Clayton VIC 3800, Australia and [4] CSIRO, Materials Science and Engineering, Clayton VIC 3168, Australia.

* Corresponding author, Phone: +61 3 9905 1762, Fax: +61 3 9905 4940, E-mail: terry.turney@monash.edu

1. Synthesis of N-[3-(triethoxysilyl)propyl]- 3,6,9,12-tetraoxatridec-1-yl ester of carbamic acid (PEGSi)

PEGSi was synthesized following a procedure from the literature with some modifications.[1] Firstly, 0.8 mL (4 mmol) of tetraethyleneglycol monomethyl ester was dissolved into 10 mL of dry pyridine with vigorous stirring under nitrogen gas flow at 70°C. After being stirred for 1 h, 1 mL (4 mmol) of 3-(triethoxysilyl)propyl isocyanate (TESPIC) was added dropwise to the mixture. The reaction was kept for 24 h at 70°C under a nitrogen atmosphere. After that, the solvent was evaporated under vacuum to afford the product as a light yellow liquid (yield 91%). ^{1}H NMR ($CDCl_3$, 400 MHz) δ: 0.59-0.63 (m, 2H), 1.20-1.23 (t, 9H), 1.57-1.66 (m, 2H), 3.14-3.19 (m, 2H), 3.37 (s, 3H), 3.53-3.56 (m, 2H), 3.63-3.67 (m, 14H), 3.78-3.84 (q, 6H), 4.19-4.21 (t, 2H). ESI-MS m/z: [M+ Na^+] = 478.3.

2. Physicochemical characterization of ZnO NPs

FTIR: Attenuated total reflection (ATR) IR spectra were collected in the region of 600-4000 cm^{-1} (resolution 4.0 cm^{-1}) on a Bruker Equinox 55 series FTIR spectrometer, with samples mounted in a diamond anvil.

SEM-EDX: Field emission gun scanning electron microscopy (FEG-SEM) was done on JEOL JSM-7001F. Samples were platinum coated and observed at an accelerating voltage of 15 keV. Energy dispersive X-ray (EDX) spectra were collected at 20keV in FEG-SEM.

XRD: Powder X-ray diffraction (XRD) patterns were recorded on a Bruker AXS D8-Advanced diffractometer with Cu Kα radiation at a scan rate of 2°/min and a step size of 0.02°.

Zeta potential: The zeta potential of the ZnO NPs in water was measured by the Zetasizer Nano-ZS from Malvern Instruments. 4 mg of ZnO NPs were dispersed in 10 mL distilled water

and then sonicated for 10 min; the pH value of the suspensions was adjusted using 0.1M HNO_3 and/or 0.1 M NaOH solutions as necessary.

TGA: Thermogravimetric analysis (TGA) employed a Mettler Toledo TGA/DSC 1 thermogravimetric analyser. All of the analyses were performed over a temperature range of 25°C - 800°C (heating rate: 10 °C/min) in air (flow rate: 120 mL/min).

XPS: X-ray photoelectron spectroscopy (XPS) and elemental analysis measurements were obtained using an AXIS Ultra DLD spectrometer (Kratos Analytical Inc., Manchester, UK) with a monochromated Al Kα source at a power of 180 W (15 kV, 12 mA). Samples were pressed into wells in a stainless steel holder. XPS peaks were referenced to C1s at 285.0 eV. Data analysis was performed with the CASAXPS software. Symmetric Gauss/Lorentz lineshapes with 30% Lorentzian contribution were used to fit the C 1s and O 1s spectra.

XRF: X-ray Fluorescence (XRF) Spectrometry measurements were performed on a Philips PW2404 Wavelength Dispersive X-ray Fluorescence Spectrometer. Samples were fused to form a lithium borate glass bead at ~1025°C.

3. Estimation of silane surface coverage of modified ZnO NPs

Estimates of the extent of silane coverage can be obtained from: 1) the bulk elemental composition of the nanomaterials (Table S1); 2) the weight loss observed by calcination of the coated nanoparticles; or 3) Si/Zn atomic ratios obtained from XPS data (Table S2).

Table S1. Si and Zn ratio in the surface modified ZnO NPs obtained from XRF measurements

Materials	**Si**		**Zn**		**Si/Zn**
	wt%	mol%	wt%	mol%	atomic ratio
ZnO@PEG	0.47	0.017	77.0	1.18	0.014
ZnO@APTES	0.96	0.034	77.0	1.18	0.029

Each calculation requires assumptions to be made that result in valid comparative values rather than absolute % surface coverages. In each case, it is assumed that the surface silane units are in the form of tripodal $RSiO_3$ units with the oxygen atoms common with the polar O-terminated $(000\bar{1})$ face of a ZnO nanoparticle, with a wurtzite structure.[2] The density of grafted silane units will be related to the density surface oxide atoms in the ZnO structure given by the known interatomic dimensions on a $(000\bar{1})$ face.

The surface area of the ZnO unit cell (0001) face, which can incorporate the tripodal $RSiO_3$ units (assuming that only (0001) faces), can be regarded as the surface area of the two hexagons in the unit cell[3] (defined as S_1), and

$$S_1 = 3\sqrt{3}r_0^2$$

Where r_0 can be regarded as the bond length of Zn-O, and the value is 198 pm. So we have

$$S_1 = \sim 2.04 \times 10^{-15}\ \text{cm}^2.$$

For a diameter of 40 nm ZnO NP, its BET surface area has been experimentally measured as S2 = 27.2 ± 1.2 m^2/g,[4] so the number of surface tripodal units in 27.2 m^2 is

$$N = \frac{S_2}{S_1} = \sim 1.33 \times 10^{20}$$

The moles of silane is

$$n_1 = \frac{N}{N_A} = \sim 2.208 \times 10^{-4}\ \text{mol}$$

Where N_A is the Avogadro's Constant (6.022×10^{23} mol^{-1}).

The atomic ratio of Si to Zn is

$$\frac{n_1}{n_2} = \frac{2.208 \times 10^{-4}}{1/81.4} = \sim 0.018$$

Based on the XRF results, the atomic ratio of Si to Zn was 0.029 and 0.014 for ZnO@APTES

and ZnO@PEG respectively, so we have the surface coverage for ZnO@APTES and ZnO@PEG as $\frac{0.029}{0.018} = 161.1\%$, and $\frac{0.014}{0.018} = 77.8\%$, respectively. A value of >100% for APTES coverage, can be ascribed either to an underestimate of available surface for silanization when measured from the BET surface area. Alternatively, formation of bridging di- or polysiloxane units (i.e. capping ligands containing Si-O-Si) could also allow for a greater incorporation of APTES than a "monolayer" coverage.

An estimate of surface silanization can also be obtained from TGA results (Figure S7), where the weight loss for bare ZnO, ZnO@APTES and ZnO@PEG was 1.375%, 2.25% and 3.25%, respectively.

The mole ratio of Si to Zn from the modified ZnO NPs is

$$\frac{n_{Si}}{n_{Zn}} = \frac{\Delta m_1 / M_1}{\Delta m_2 / M_2} \quad \text{(eq. 1)}$$

Where Δm_1 and Δm_2 is the residue weight of ligand and ZnO NPs respectively, and M_1 and M_2 stand for the molecular weight of residue ligand and ZnO NPs, respectively. It is assumed that heating the silanized samples in air will result in the silane converting exclusively into SiO_2, without its altering the ZnO stoichiometry.

According to equation 1, for ZnO@APTES, we have

$$\frac{n_{Si}}{n_{Zn}} = \frac{(98.625\% - 97.75\%)/58.10}{97.75\%/81.408} = 0.0125$$

Similarly, for ZnO@PEG NPs, we have

$$\frac{n_{Si}}{n_{Zn}} = \frac{(98.625\% - 96.75\%)/292.35}{96.75\%/81.408} = 0.0054$$

Finally, we have the surface coverage for ZnO@APTES and ZnO@PEG as $\frac{0.0125}{0.018} = 69.4\%$, and $\frac{0.0054}{0.018} = 30.0\%$, respectively. The loss of weight on heating for the bare ZnO sample is partly ascribed to loss of adsorbed carbonate and water, as well as to the reversible loss of oxygen as the ZnO nanoparticles are heated. It is well known that ZnO may become non-

stoichiometric upon heating.[5] This estimation of surface coverage is, thus, also prone to uncertainty, as it is not known how silanization will alter the other surface species or rate of de-oxygenation of the ZnO.

Calculation of silane surface coverage based on XPS data was not attempted as it was not possible to estimate the level of surface Zn from the Zn 2p3/2 data. The attenuation of the Zn photoelectron signal will follow a Beer's Law relationship dependent upon the X-ray penetration depth, which is difficult to estimate. However, it is worth noting that the Si/Zn atomic ratio from the XPS for ZnO@APTES was about twice that for the ZnO@PEG sample (Table S2). Thus, differences in surface coverage percentages calculated from XRF, XPS and TGA results are expected to differ as a result of the assumptions required. However, the relatively greater silane surface coverage of ZnO@APTES over that of ZnO@PEG was consistent, when measure by each method.

4. UV–Vis absorption spectrum of ZnO NPs

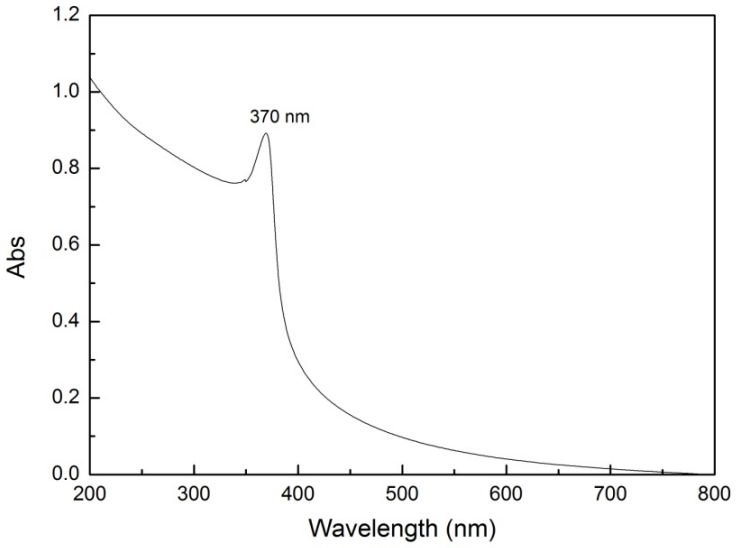

Figure S1. UV–Vis absorption spectrum of bare ZnO NPs in water (1 mM)

4. FTIR Spectra

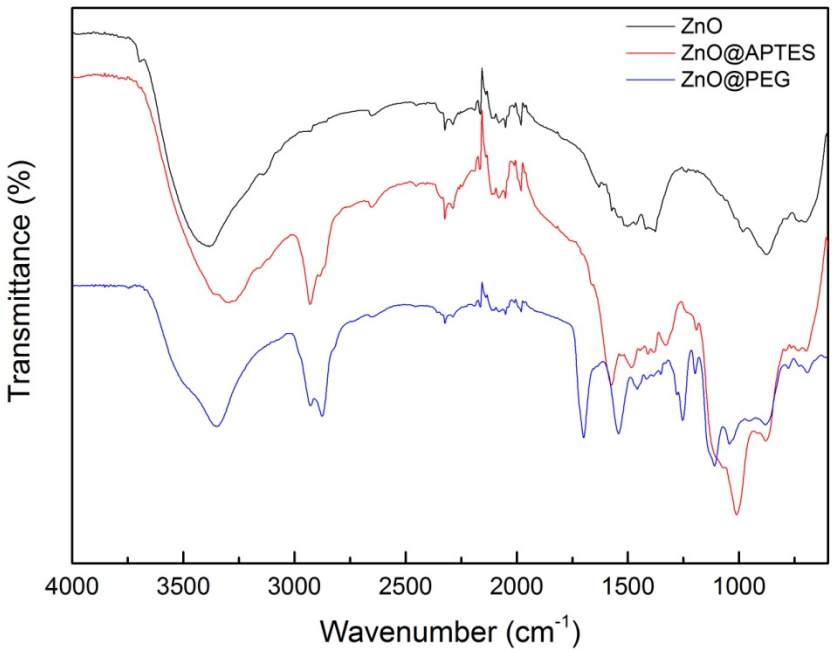

Figure S2. FTIR spectra of bare and modified ZnO NPs.

5. Scanning Electron Microscopy

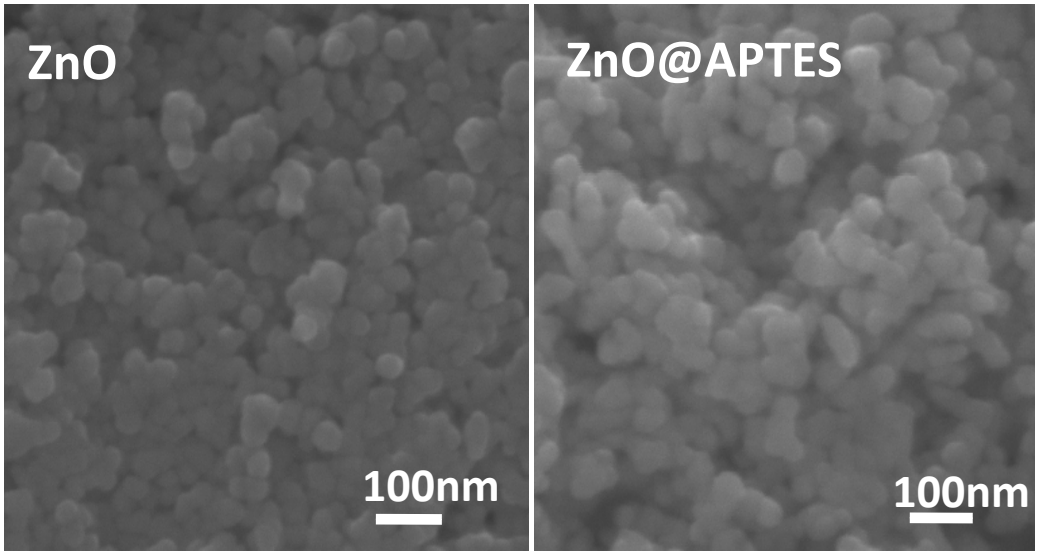

Figure S3. SEM images of ZnO and ZnO@APTES NPs.

6. XRD Powder Patterns

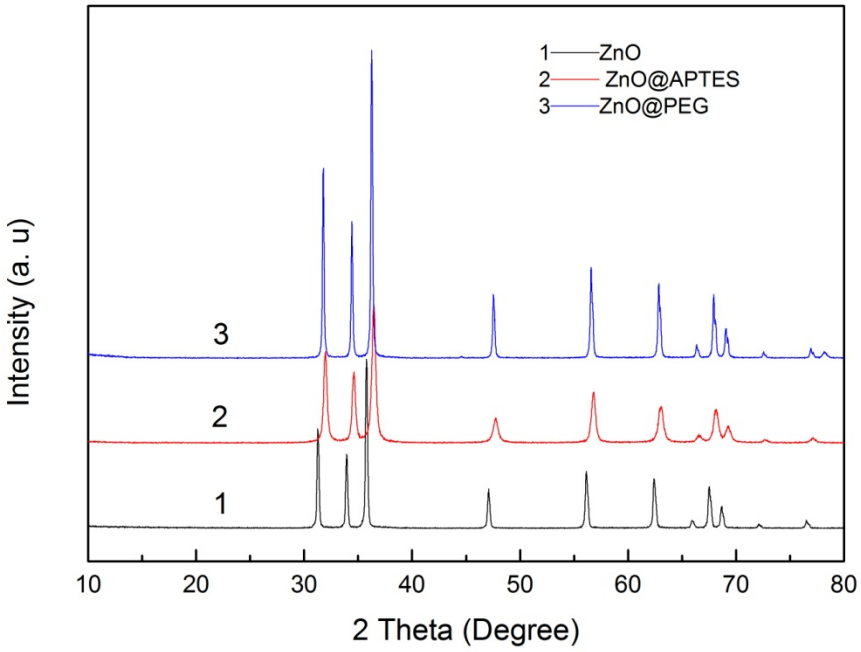

Figure S4. XRD patterns of bare and modified ZnO NPs.

7. X-ray Photoelectron Spectra

XPS survey spectra are shown in Figure S5, with atomic binding energies and atomic ratios presented in Tables S2 and S3, respectively. The binding energies have been adjusted to a C 1s (C-C) binding energy of 285.0 eV. The Zn 2p3/2 was typical of Zn^{2+}. The Zn 2p3/2 binding energy is relatively insensitive to local chemical environment and provides no additional information on the local chemistry. The high resolution Si 2p spectra are shown in Figure S6. The C 1s spectrum was fitted with 3 components with the lower component (285.0 eV) being related to adventitious carbon in the case of the ZnO NPs, but there is an additional C-C from the APTES with the other two samples. There are also additional components at 286.0 to 286.8 eV, and in the vicinity of 289.0 eV. The peak in the region of 286.0 to 286.8 eV is normally associated with a single C-O bond, but its origin is not clear in the unmodified ZnO

nanoparticle powder, as it is too low for reported values for bicarbonate, but may be due to traces of residual solvent. In the other two cases it is associated with the organics from the amino silane and PEGSi. The highest binding energy C 1s is associated with surface carbonate/bicarbonate. The O 1s has been fitted with two components; the lower one for the oxide (530.1 eV) and the higher one accounts for both hydroxyl ions as well as carbonate ions. The higher O 1s peak could be further fitted with components to account for the hydroxyl and carbonate moieties separately.

As would be expected, the O/Zn ratio increased for the two treated surfaces, reflecting an increased O signal from the surface treatment and perhaps some attenuation of the Zn signal. This trend was also the same for the C/Zn atomic ratios. The Si/Zn ratio for the APTES treatment is around twice of the ratio for the silane/PEG treatment. The N/Si ratio was higher than would be expected on the basis of the stoichiometry which is 1:1, although this might be explained by some attenuation if all the silane is bonded vertically to the surface via the Si. Finally, the C-C to carbonate ratio increases with all treatments, but for the silane/PEG the ratio is nearly double that for the APTES ratio. It is not clear whether all this increase is due to the PEG or whether CO_3^{2-} has been partially removed.

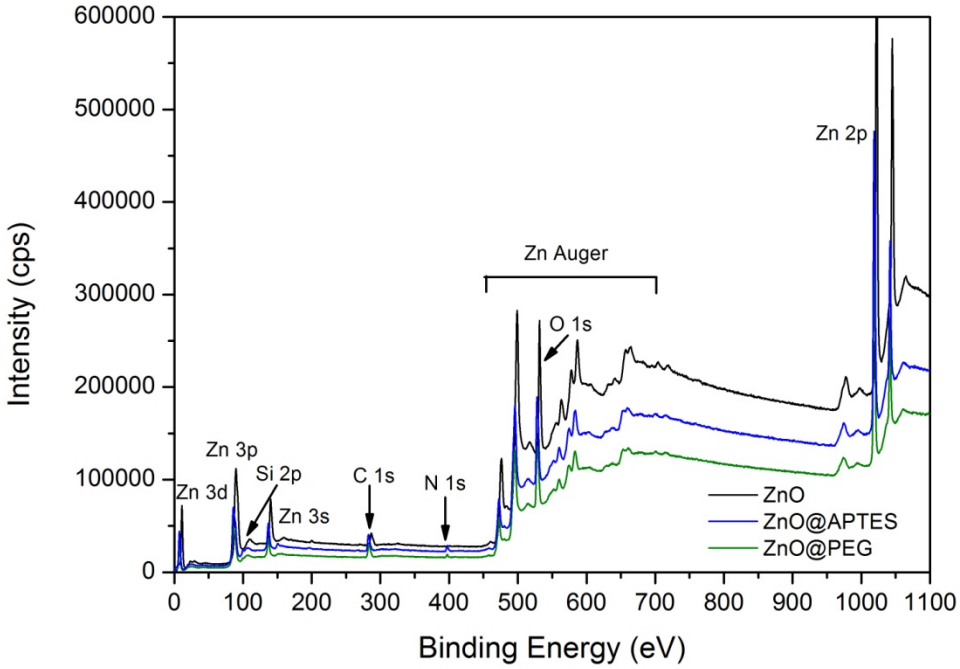

Figure S5. XPS survey scans of the bare and modified ZnO NPs showing various Zn peaks as well as O 1s, N 1s, C 1s and Si 2p peaks.

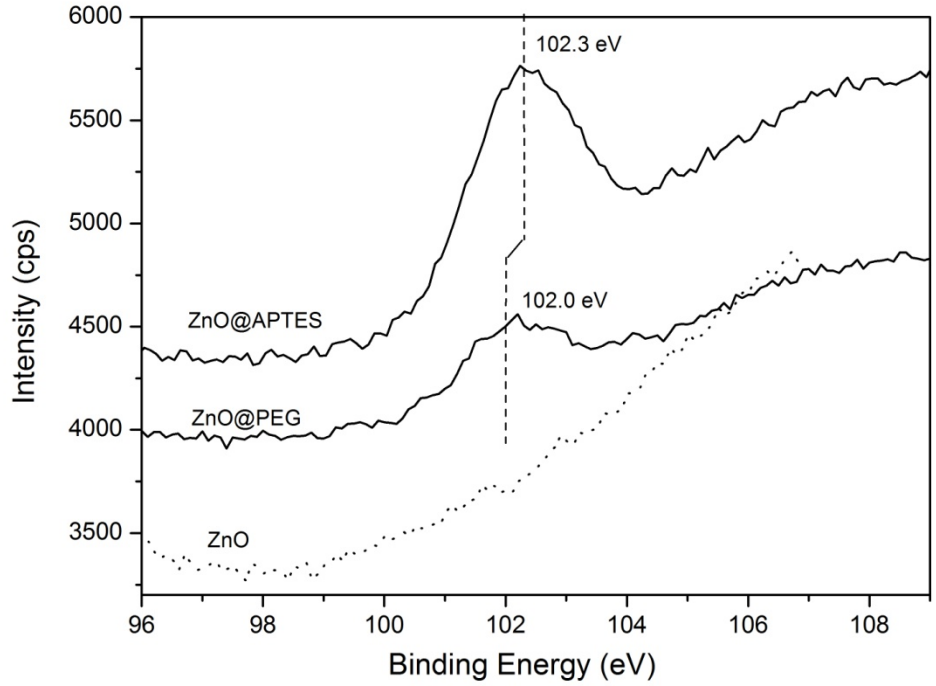

Figure S6. High resolution Si 2p peaks for bare and modified ZnO NPs. The Si 2p binding energies have been corrected using a C 1s line position of 285.0 eV. The binding energies are typical of silanes. No Si was detected on the ZnO sample.

Table S2: XPS binding energies of bare and surface modified ZnO NPs

Materials	**Zn 2p3/2**	**Si 2p**	**C 1s C-C**	**C 1s C-O**	**C1s CO_3^{2-}**	**O 1s ox**	**O 1s HBE**
ZnO	1021.4	-	285.0	286.6	288.9	530.1	531.6
ZnO@APTES	1021.4	102.3	285.0	286.2	288.7	530.2	531.7
ZnO@PEG	1021.3	102.0	285.0	286.8	289.4	530.3	532.1

Table S3. XPS Atomic ratios of bare and surface modified ZnO NPs

Sample	**O/Zn**	**Si/Zn**	**C /Zn**	**N/Si**	**O/C**	**C-C/CO_3^{2-}**
ZnO	1.58	-	0.49	-	3.24	2.05
ZnO@APTES	2.30	0.0772	1.21	1.57	1.89	2.51
ZnO@PEG	2.18	0.038	1.17	1.44	1.87	4.12

8. Thermogravimetric Data

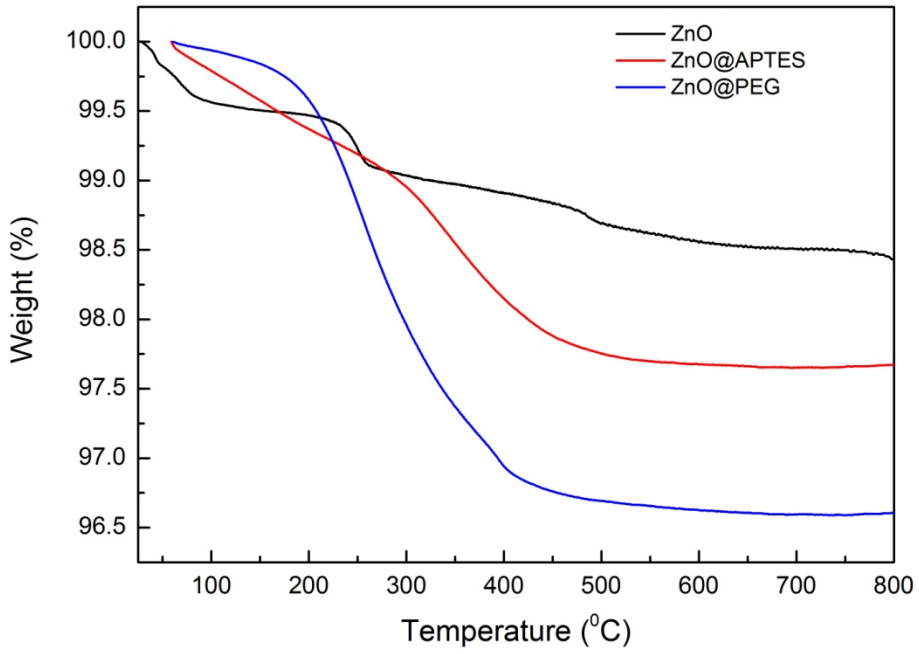

Figure S7. TGA of bare and modified ZnO NPs.

9. Table S4. Chemical composition of artificial lysosomal fluid (ALF, pH 4.5)

Chemicals	Concentration (g/L)
Magnesium chloride ($MgCl_2$)	0.05
Sodium chloride (NaCl)	3.21
Disodium phosphate (Na_2HPO_4)	0.071
Sodium sulfate (Na_2SO_4)	0.039
Calcium chloride dihydrate ($CaCl_2{\cdot}2H_2O$)	0.128
Trisodium citrate dihydrate ($C_6H_5Na_3O_7{\cdot}2H_2O$)	0.077
Sodium hydroxide (NaOH)	6.0
Citric acid ($C_6H_8O_7$)	20.8
Glycine (H_2NCH_2COOH)	0.059
Disodium tartrate dihydrate ($C_4H_4O_6Na_2{\cdot}2H_2O$)	0.09
Sodium lactate ($C_3H_5NaO_3$)	0.085
Sodium pyruvate ($C_3H_3O_3Na$)	0.086

References

1 Q. He, J. Zhang, J. Shi, Z. Zhu,L. Zhang, W. Bu, L. Guo and Y. Chen, Biomaterials, 2010, **31**, 1085.

2 A. Wander, F. Schedin, P. Steadman, A. Norris, R. McGrath, T.S. Turner, G. Thornton and N.M. Harrison, Phys. Rev. Lett., 2001, **86**, 3811.

3 C. M. Schlepütz, Y. Yang, N. S. Husseini, R. Heinhold, H. S. Kim, M. W. Allen, S. M. Durbin and R. Clarke, J. Phys.: Condens. Matter 2012, **24**, 095007

4 C. Singh, S. Friedrichs, M. Levin, R. Birkedal, K. Jensen, G. Pojana, W. Wohlleben, S. Schulte, K. Wiench and T. Turney, EUR Report, 2011, 25066.

5 H. J. Allsopp and J. P. Roberts, Trans. Faraday Soc., 1959, **55**, 1386.